ORIGINAL ARTICLE

Hidden diversity revealed by genome-resolved metagenomics of iron-oxidizing microbial mats from Lō'ihi Seamount, Hawai'i

Heather Fullerton[1], Kevin W Hager, Sean M McAllister[2] and Craig L Moyer
Department of Biology, Western Washington University, Bellingham, WA, USA

The Zetaproteobacteria are ubiquitous in marine environments, yet this class of Proteobacteria is only represented by a few closely-related cultured isolates. In high-iron environments, such as diffuse hydrothermal vents, the Zetaproteobacteria are important members of the community driving its structure. Biogeography of Zetaproteobacteria has shown two ubiquitous operational taxonomic units (OTUs), yet much is unknown about their genomic diversity. Genome-resolved metagenomics allows for the specific binning of microbial genomes based on genomic signatures present in composite metagenome assemblies. This resulted in the recovery of 93 genome bins, of which 34 were classified as Zetaproteobacteria. Form II ribulose 1,5-bisphosphate carboxylase genes were recovered from nearly all the Zetaproteobacteria genome bins. In addition, the Zetaproteobacteria genome bins contain genes for uptake and utilization of bioavailable nitrogen, detoxification of arsenic, and a terminal electron acceptor adapted for low oxygen concentration. Our results also support the hypothesis of a Cyc2-like protein as the site for iron oxidation, now detected across a majority of the Zetaproteobacteria genome bins. Whole genome comparisons showed a high genomic diversity across the Zetaproteobacteria OTUs and genome bins that were previously unidentified by SSU rRNA gene analysis. A single lineage of cosmopolitan Zetaproteobacteria (zOTU 2) was found to be monophyletic, based on cluster analysis of average nucleotide identity and average amino acid identity comparisons. From these data, we can begin to pinpoint genomic adaptations of the more ecologically ubiquitous Zetaproteobacteria, and further understand their environmental constraints and metabolic potential.
The ISME Journal (2017) **11**, 1900–1914; doi:10.1038/ismej.2017.40; published online 14 April 2017

Introduction

Microbes are everywhere, and in many ecosystems they are the key drivers of biogeochemical cycles. Iron is the most abundant element in the earth and only microbes are able to utilize it as an energy source. Mineralogical evidence of iron- oxidizers has been found, dating to 1.89 Ga, making iron oxidation a very ancient metabolism (Planavsky *et al.*, 2009). Early Earth hosted a ferruginous ocean where iron oxidation may have been the dominant metabolism (Ilbert and Bonnefoy, 2013; Guilbaud *et al.*, 2015). Microbial iron oxidizers are found suspended in the water column (Field *et al.*, 2016), but extensive microbial growth by iron oxidation is limited to areas of high ferrous iron and low oxygen concentrations, such as hydrothermal vents (Emerson and Moyer, 2010; Scott *et al.*, 2015).

Reduced iron released by hydrothermal vent systems fuels primary production by lithoautotrophic microbes, which in turn support additional trophic levels making hydrothermal vent systems some of the most biologically active regions of the deep-sea (Sievert and Vetriani, 2012). It is estimated that 3×10^{11} mol of Fe(II) is released each year through hydrothermal venting in Earth's oceans (Holland, 2006), and is transported in the water column thousands of kilometers away from the source (Resing *et al.*, 2015), where it can be utilized by phototrophs in the upper ocean; however, iron is still a limiting factor for phototrophs in the upper ocean (Raven *et al.*, 1999). The abiotic oxidation of Fe(II) by O_2 is rapid in fully aerated seawater (Konhauser *et al.*, 2005; Druschel *et al.*, 2008). Therefore, from a microbe's perspective, Fe(II) is potentially a vast food source, yet it is as ephemeral as it is abundant and bioavailable.

Microbial iron oxidation has been recognized in freshwater systems since the 1890s, whereas microbial iron oxidation in marine systems is just

Correspondence: C Moyer, Department of Biology, Western Washington University, 516 High Street, MS# 9160, Bellingham, WA 98225, USA.
E-mail: cmoyer@hydro.biol.wwu.edu
[1]Current address: Department of Biology, Pacific Lutheran University, Tacoma, WA, USA
[2]Current address: Department of Geological Sciences and School of Marine Science and Policy, University of Delaware, Newark, DE, USA

beginning to be recognized (Emerson et al., 2013; Fleming et al., 2013). The isolates of the newest class of Proteobacteria, the Zetaproteobacteria, are described as neutrophilic marine iron-oxidizers (Emerson et al., 2007). Zetaproteobacteria have been identified throughout the Pacific and Atlantic Oceans at hydrothermal vent habitats and estuaries (McAllister et al., 2011; Scott et al., 2015; Field et al., 2016). At sites where the predominant vent effluent is high in ferrous iron, Zetaproteobacteria are the dominant microbial mat community members, with the classes of the Gamma-, Delta- and Epsilon-proteobacteria as well as Nitrospira consistently detected in these habitats (Moyer et al., 1995; Rassa et al., 2009; Fleming et al., 2013). Several Zetaproteobacteria operational taxonomic units have been identified and two are globally ubiquitous in iron-driven microbial mat communities (McAllister et al., 2011).

Zetaproteobacteria are considered ecosystem engineers due to their foundational role in the formation of the microbial mat architecture. This architecture is comprised of exopolysaccharide structures, including twisted helical stalks or tubular sheaths as observed by microscopic analysis of cultures and microbial mats (Chan et al., 2011; Fleming et al., 2013; Chan et al., 2016b). Through the production of stalks or sheaths, the Zetaproteobacteria can alter their physical and chemical environment (Chan et al., 2016a). Furthermore, Zetaproteobacteria are lithoautotrophs and the primary producers in iron-dominated hydrothermal vent systems (Singer et al., 2011; Field et al., 2015). Previous molecular analysis of microbial mats at Lōʻihi Seamount showed that Zetaproteobacteria correlate with the abundance of key functional genes, but that functional gene abundance did not vary across varying mat morphologies; furthermore, vent chemistry was found to be associated with the observed mat morphologies (Jesser et al., 2015), suggesting unrealized genomic diversity within the Zetaproteobacteria.

Zetaproteobacteria were first described at Lōʻihi Seamount, which is located 35 km south-east of the big island of Hawaiʻi and hosts a plethora of dynamic hydrothermal vents (Moyer et al., 1995). In 1996, a major eruption formed Pele's Pit, a 300 m wide caldera near the summit, with several active hydrothermal venting sites (Figure 1). Before the 1996 eruption, Lōʻihi was dominated by low-temperature diffuse-flow hydrothermal vents emitting fluids up to ~ 70 °C and elevated levels of Fe(II), CO_2, CH_4 and NH_4^+ (Sedwick et al., 1992; Wheat et al., 2000) and has now returned to these pre-eruption conditions (Glazer and Rouxel, 2009).

Biogeographic patterns for marine microbes remain poorly understood in terms of distribution scale and evolutionary divergence rates. To address this, we sequenced six distinct microbial mat communities collected from Lōʻihi Seamount. From this, a shotgun metagenomics approach was used,

where we were able to construct a composite assembly for genome binning. We used differential coverage analysis to reconstruct site-specific community composition and compared this to the community structure as determined by taxa specific Quantitative PCR (qPCR) analyses. Here we present genome-resolved metagenomics to further explore patterns of biodiversity and adaptation of Zetaproteobacteria populations, including two ecologically significant Zetaproteobacteria OTUs (zOTUs).

Materials and methods

Sample collection
Microbial mat samples were collected at Lōʻihi Seamount, HI in October 2009 by the remotely operated vehicle (ROV) Jason II onboard the R/V Kilo Moana. Samples were collected from within Pele's Pit at Hiolo North (Markers 31, 36 and 39), Hiolo South (Markers 34 and 38), and Kuʻkulu Base (no marker) or on the caldera rim at Pohaku (Marker 57) (Figure 1). All samples were collected using a single-action Biomat Syringe (BS) sampler (Figure 2c) as described in Fleming et al. (2013).

DNA extraction, T-RFLP analysis, and qPCR
Genomic DNA was extracted from samples using the FastDNA SPIN kit for soil (MP Biomedical, Santa Ana, CA, USA) according to manufacturer's protocol. Cells were lysed by bead beating twice (stored on ice for 5 min in between) in a FastPrep instrument (MP Biomedical) at a speed setting of 5.5 for 45 s and DNA was eluted with 1 mM Tris at pH 8. Genomic DNA was quantified with a Qubit 2.0 fluorometer (ThermoFisher Scientific, Waltham, MA, USA).

Samples were PCR amplified for use in terminal-restriction fragment length polymorphisms (T-RFLP) as previously described (Davis and Moyer, 2008). PCR was visualized on a 1% agarose gel before restriction digestion. The end-labeled fragments were run on an ABI model 3130XL automated DNA sequencer and the data were analyzed with the BioNumerics v7.6 software (Applied Maths, Austin, TX, USA). SSU rRNA gene clone libraries from five sampled microbial mat communities were constructed as described in McAllister et al. (2011), in order assess putative phylotypes in the T-RFLP dataset (Supplementary Figures 1 and 2).

qPCR conditions along with Bacterial and Zetaproteobacterial primers used were the same as described by Jesser et al. (2015). Zetaproteobacteria abundance was determined using the ratio of Zetaproteobacteria to Bacteria SSU rRNA gene copies per nanogram gDNA. No qPCR data were used unless primers exhibited better than 95%
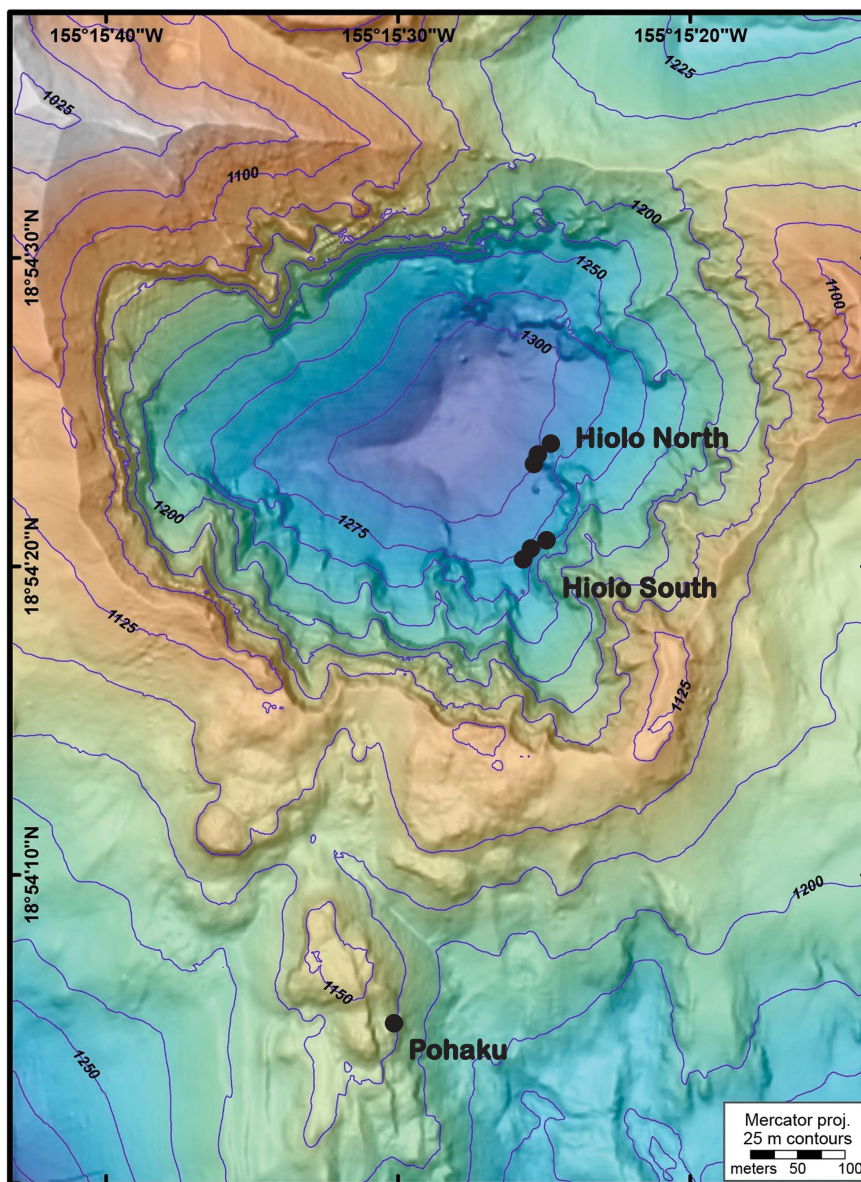
Figure 1 Bathymetric map (high resolution at < 2 m) of sampling sites in and near Pele's Pit caldera on the summit of Lō'ihi Seamount, Hawai'i. Precise marker locations include Pohaku (Marker 57), Hiolo North (Markers 36, 39 and 31), Hiolo South (Markers 34, 38 and Ku'kulu). Courtesy of Susan Merle, NOAA EOI/OSU.

efficiency and yielded single-peak amplicons upon post-PCR melt curve analysis.

Metagenomic sequencing, assembly and annotation
Extracted DNA was cleaned and concentrated using an Aurora (Boreal Genomics, Vancouver, BC, Canada) prior to sequencing; libraries were prepared with the Nextera DNA Library Kit (Illumina, San Diego, CA, USA). Sample J2-479-BS3 was run on an Illumina HiSeq 2000 using paired-end sequencing with reads of 101 bp from each end. Sample J2-483-BS63 was run using paired-end sequencing with reads of 84 bp on an Illumina MiSeq and was a combination of two samples

collected from the same microbial mat. The remainder of the samples were run using an Illumina MiSeq with paired-end sequencing of 308 bp reads (Supplementary Table 1).

Sequenced reads were quality checked using FastQC (Andrews, 2010) and were trimmed of adaptors, and pairs were matched using cutadapt (Martin, 2011). Trimmed reads were normalized using BBnorm (target depth: 18). The resulting reads were assembled with IDBA-UD (Peng *et al.*, 2012) (k-mer sizes: 50–240 in steps of 10 without correction). Reads from each sample were mapped, with bowtie2 (Langmead and Salzberg, 2012) to the composite assembly to get coverage information. This was then used to construct genome bins with MaxBin 2.0 (Wu *et al.*,
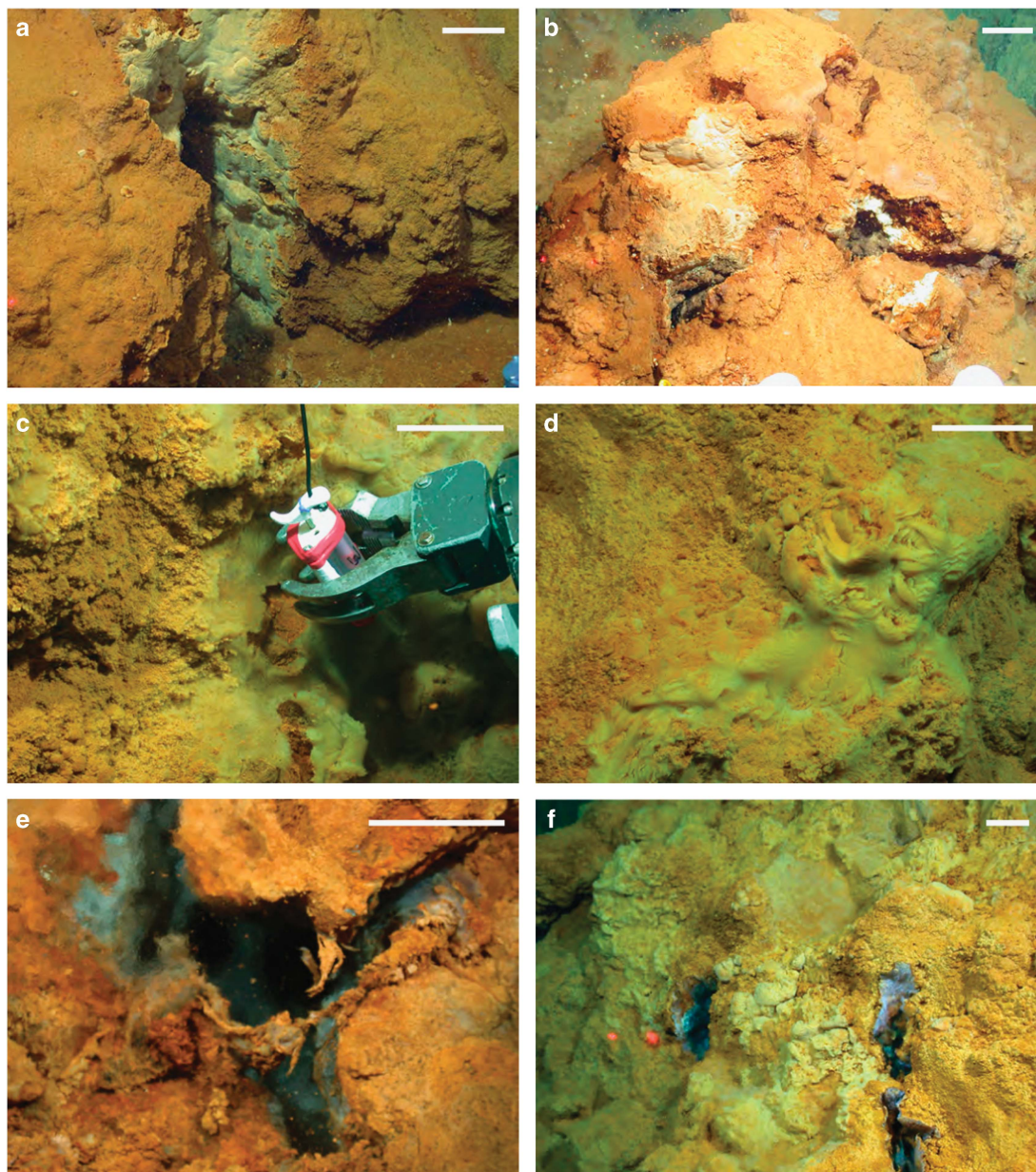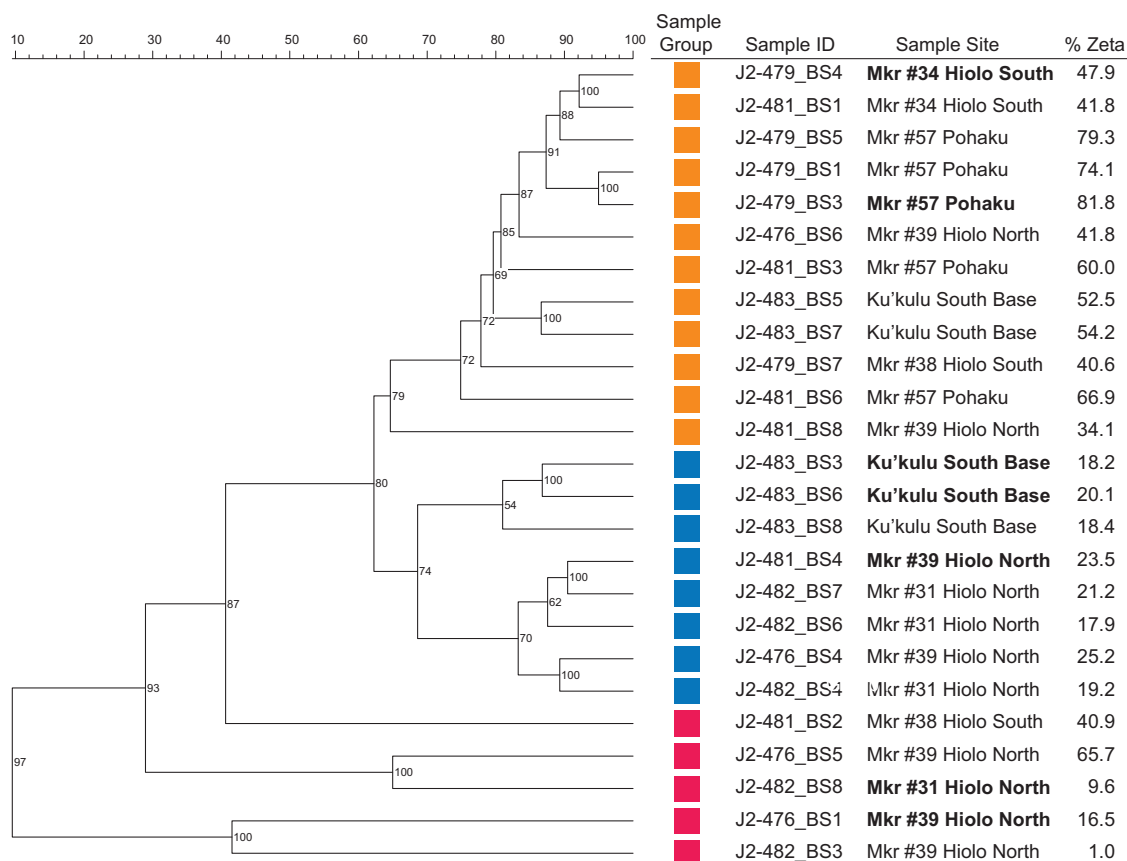
Figure 2 Photos illustrating the different mat morphologies. (**a**) curd-type mat from Marker 34, (**b**) curd-type mat from Marker 57, (**c**) veil-type mat from Ku'kulu, (**d**) veil-type mat from Marker 39, (**e**) streamers from Marker 31, and (**f**) streamers from Marker 39. Scale bars are 10 cm.

2016) using default parameters. The resulting genome bins were evaluated with CheckM (Parks et al., 2015). The assembled composite metagenome was uploaded to Integrated Microbial Genomics (IMG) for annotation. Genome bins were separated from bulk data after annotation.

Genes annotated as specific proteins identified in *M. ferrooxydans* PV-1 were identified by BLASTp searches of the composite metagenome with an *e*-value cutoff of 10^{-5} (Supplementary Tables 2). $Cyc1_{PV-1}$ (DAA64808.1), and $Cyc2_{PV-1}$ (AKN35166.1) were identified via proteomics (Barco et al., 2015) and Mob (SPV1_03948) identified

via fosmid library genome analysis (Singer et al., 2011).

Average nucleotide and average amino acid identities
Genome bins identified as Zetaproteobacteria by CheckM were compared to genome sequences of Zetaproteobacteria single amplified genomes (SAGs) and Zetaproteobacteria isolate genomes. The average nucleotide identity (ANI) was calculated using the BLAST-based algorithm tool in JSpecies v1.2.1 (Richter and Rosselló-Móra, 2009). The average amino acid identity was calculated using the

Scale	Sample Group	Sample ID	Sample Site	% Zeta
	orange	J2-479_BS4	**Mkr #34 Hiolo South**	47.9
	orange	J2-481_BS1	Mkr #34 Hiolo South	41.8
	orange	J2-479_BS5	Mkr #57 Pohaku	79.3
	orange	J2-479_BS1	Mkr #57 Pohaku	74.1
	orange	J2-479_BS3	**Mkr #57 Pohaku**	81.8
	orange	J2-476_BS6	Mkr #39 Hiolo North	41.8
	orange	J2-481_BS3	Mkr #57 Pohaku	60.0
	orange	J2-483_BS5	Ku'kulu South Base	52.5
	orange	J2-483_BS7	Ku'kulu South Base	54.2
	orange	J2-479_BS7	Mkr #38 Hiolo South	40.6
	orange	J2-481_BS6	Mkr #57 Pohaku	66.9
	orange	J2-481_BS8	Mkr #39 Hiolo North	34.1
	blue	J2-483_BS3	**Ku'kulu South Base**	18.2
	blue	J2-483_BS6	**Ku'kulu South Base**	20.1
	blue	J2-483_BS8	Ku'kulu South Base	18.4
	blue	J2-481_BS4	**Mkr #39 Hiolo North**	23.5
	blue	J2-482_BS7	Mkr #31 Hiolo North	21.2
	blue	J2-482_BS6	Mkr #31 Hiolo North	17.9
	blue	J2-476_BS4	Mkr #39 Hiolo North	25.2
	blue	J2-482_BS4	Mkr #31 Hiolo North	19.2
	red	J2-481_BS2	Mkr #38 Hiolo South	40.9
	red	J2-476_BS5	Mkr #39 Hiolo North	65.7
	red	J2-482_BS8	**Mkr #31 Hiolo North**	9.6
	red	J2-476_BS1	**Mkr #39 Hiolo North**	16.5
	red	J2-482_BS3	Mkr #39 Hiolo North	1.0

Figure 3 T-RFLP analysis of BioMat Samples collected from Lōʻihi microbial mats. Colored boxes represent the three different groups that resulted from the cluster analysis: Group I, orange; Group II, blue; Group III, red. The sampled mat communities in bold were selected for Illumina metagenomic sequencing.

enveomics toolbox (Rodriguez-R and Konstantinidis, 2016). Hierarchical cluster analysis was calculated in R using the gplots package.

Phylogenetic analysis
All genes annotated as a ribulose 1,5-bisphosphate carboxylase (RubisCO) were further analyzed for binning and taxonomic placement. IMG phylogeny was used for the unbinned genes, whereas CheckM was used for the genes within a genome bin. The identified RubisCO Form II amino acid sequences were then aligned using the Geneious v9.1 aligner (Kearse *et al.*, 2012). The resulting alignments were manually screened, and all sequences less than 110 amino acids were removed from analysis. The resulting alignment was then used to create a phylogenic consensus tree with RAxML v7.2.8 using the gamma GTR protein model with 1000 bootstrap iterations, again with Geneious (Kearse *et al.*, 2012).

Accession numbers
Representative sequences from each operational taxonomic unit identified in the clone libraries were submitted to GenBank. Accession numbers

are JQ287646–JQ287657, JX468894 (Fleming *et al.*, 2013) and KY417831–KY417866 (this study). All metagenomic contigs have been made available in the IMG Database (IMG Genome ID 3300009408). All sequence data are also available from NCBI SRA (Biosample accessions SAMN06226859-SAMN06226864).

Results and Discussion

Site description and community structure
Microbial mats vary in and around Pele's Pit in gross morphology and color, from white-yellow to burnt orange (Figures 2a–f). In addition to variation in color, the mats had variable textures that were assigned to three specific mat morphological groups associated with variable fluid flow regimes. These were described as curds in the presence of direct flow (Figures 2a and b), veils associated with diffuse flow (Figures 2c and d), and streamers also found in direct flow (Figures 2e and f). Pohaku is the only sample site located on the outside of Pele's Pit on the southern rim of this caldera (Figure 1), and has been characterized as highest in reduced iron, at nearly 1 mM (Glazer and Rouxel, 2009). Microscopic analysis of the curd-type mat shows the

Table 1 Summary statistics of 77 population genomes, which have been assigned to a phylogenetic class

Bin Id	Class	GC Content (%)	Genome size (Mbp)	Gene count	Compl. (%)	Cont. (%)	Scaffolds (no.)	Longest scaffold (bp)
ZetaBin011	Zetaproteobacteria	58.51	2.14	2472	96.64	2.43	305	50 762
ZetaBin022	Zetaproteobacteria	55.75	2.27	3048	83.51	12.68	1107	17 841
ZetaBin030	Zetaproteobacteria	49.62	0.14	202	9.40	0.00	57	8654
ZetaBin035	Zetaproteobacteria	60.80	2.92	3306	94.26	22.37	525	99 453
ZetaBin037	Zetaproteobacteria	58.78	1.98	2929	33.29	9.66	1254	16 849
ZetaBin040	Zetaproteobacteria	47.98	2.91	2812	98.74	0.84	145	144 433
ZetaBin041	Zetaproteobacteria	50.51	2.19	2391	96.80	12.77	321	43 694
ZetaBin042	Zetaproteobacteria	51.09	2.64	2707	97.06	3.21	188	129 034
ZetaBin043	Zetaproteobacteria	50.12	1.90	2339	63.98	5.43	538	25 129
ZetaBin047	Zetaproteobacteria	51.36	3.18	4581	73.66	33.61	1364	25 119
ZetaBin049	Zetaproteobacteria	52.24	2.65	3747	72.41	26.54	955	18 206
ZetaBin050	Zetaproteobacteria	51.42	3.33	4118	95.66	18.26	600	76 915
ZetaBin052	Zetaproteobacteria	43.64	0.60	682	22.86	0.05	146	16 046
ZetaBin055	Zetaproteobacteria	43.43	0.75	909	40.87	0.14	221	11 516
ZetaBin056	Zetaproteobacteria	43.77	0.64	837	26.42	3.09	247	12 705
ZetaBin057	Zetaproteobacteria	43.16	0.45	625	19.75	1.72	202	10 079
ZetaBin058	Zetaproteobacteria	43.59	0.33	438	14.11	0.19	153	11 627
ZetaBin059	Zetaproteobacteria	42.76	0.71	956	30.09	9.80	275	11 729
ZetaBin060	Zetaproteobacteria	42.09	0.41	587	6.55	0.34	180	7595
ZetaBin062	Zetaproteobacteria	43.75	0.62	783	34.87	0.00	216	11 379
ZetaBin064	Zetaproteobacteria	43.02	0.73	953	18.26	0.00	304	16 336
ZetaBin065	Zetaproteobacteria	41.82	4.32	5575	78.50	34.27	1556	27 653
ZetaBin066	Zetaproteobacteria	48.52	3.69	4265	99.58	5.46	541	87 185
ZetaBin069	Zetaproteobacteria	42.71	0.79	1109	10.27	0.69	342	10 884
ZetaBin077	Zetaproteobacteria	50.37	2.17	2648	93.63	16.43	738	17 579
ZetaBin078	Zetaproteobacteria	43.08	0.50	702	19.48	0.00	259	9548
ZetaBin079	Zetaproteobacteria	51.17	2.24	2521	86.27	10.85	365	24 239
ZetaBin080	Zetaproteobacteria	47.96	2.96	3001	96.22	15.64	280	89 556
ZetaBin084	Zetaproteobacteria	49.43	4.46	5555	95.77	36.35	2073	22 352
ZetaBin088	Zetaproteobacteria	52.51	2.94	3356	90.99	22.27	827	30 533
ZetaBin089	Zetaproteobacteria	46.84	7.73	8861	98.59	55.28	2338	145 501
ZetaBin090	Zetaproteobacteria	44.39	2.66	3080	91.22	22.57	836	26 177
ZetaBin091	Zetaproteobacteria	43.81	1.60	2257	59.55	3.32	900	7813
ZetaBin092	Zetaproteobacteria	48.98	2.19	2486	90.17	8.05	579	33 624
PlanctoBin028	Planctomycetia	70.38	2.53	3027	66.15	18.11	1153	15 570
PlanctoBin046	Planctomycetia	56.90	3.93	5336	59.95	29.64	2392	62 755
NitroBin001	Nitrospira	42.82	2.70	2876	100.00	2.73	145	102 379
NitroBin004	Nitrospira	49.60	2.94	3178	91.13	3.52	423	72 390
NitroBin006	Nitrospira	55.00	2.97	2728	97.41	1.72	107	231 086
NitroBin008	Nitrospira	54.70	3.51	3231	99.08	2.44	130	308 593
NitroBin010	Nitrospira	48.18	1.27	1628	10.85	0.16	525	19 238
NitroBin051	Nitrospira	66.96	1.91	2303	59.18	1.72	873	9924
IgnaviBin015	Ignavibacteria	34.92	4.28	4351	100.00	22.15	792	62 071
GemmaBin005	Gemmatimonadetes	65.73	3.33	2732	97.80	1.10	93	433 639
GemmaBin009	Gemmatimonadetes	70.00	3.08	2652	100.00	1.10	139	186 026
GammaBin013	Gammaproteobacteria	62.84	3.47	3308	97.46	4.56	366	92 648
GammaBin018	Gammaproteobacteria	64.56	3.40	3474	98.28	10.53	449	84 061
GammaBin021	Gammaproteobacteria	64.89	1.72	2122	61.34	2.37	470	21 092
GammaBin025	Gammaproteobacteria	63.75	2.91	3074	97.56	7.71	383	39 220
GammaBin034	Gammaproteobacteria	45.52	3.17	4017	97.93	21.32	1080	37 727
GammaBin036	Gammaproteobacteria	55.82	3.34	4213	68.97	18.28	1152	33 248
GammaBin038	Gammaproteobacteria	60.57	5.80	6109	93.89	83.17	1221	60 894
GammaBin045	Gammaproteobacteria	60.12	1.96	2816	72.49	22.73	1122	9308
GammaBin063	Gammaproteobacteria	43.85	1.44	2097	22.48	0.79	507	197 530
GammaBin076	Gammaproteobacteria	50.35	3.06	3378	95.77	8.63	588	44 851
GammaBin082	Gammaproteobacteria	42.31	3.44	3647	88.17	5.25	565	52 724
GammaBin093	Gammaproteobacteria	38.54	4.19	4496	97.06	3.98	476	90 958
FlavoBin054	Flavobacteriia	40.70	1.45	2303	17.41	2.47	812	27 641
FlavoBin072	Flavobacteriia	30.74	2.76	3716	67.07	22.79	1138	21 266
FlavoBin087	Flavobacteriia	29.74	3.28	3737	78.86	37.63	543	33 162
EpsilonBin027	Epsilonproteobacteria	31.35	3.20	4464	91.12	40.00	1399	17 806
EpsilonBin032	Epsilonproteobacteria	38.78	1.83	2035	96.67	6.35	226	62 498
EpsilonBin033	Epsilonproteobacteria	35.69	1.33	1883	33.03	5.34	669	22 159
EpsilonBin053	Epsilonproteobacteria	38.02	1.49	1694	95.90	4.17	243	33 983
EpsilonBin071	Epsilonproteobacteria	38.65	2.82	3865	51.40	18.20	1184	37 928
DeltaBin002	Deltaproteobacteria	62.33	3.07	2716	98.21	1.21	268	89 342
DeltaBin003	Deltaproteobacteria	56.12	2.31	2081	94.19	2.80	105	128 268
DeltaBin016	Deltaproteobacteria	72.27	6.62	4801	89.52	4.19	561	102 686
DeltaBin031	Deltaproteobacteria	54.46	2.27	2924	64.58	11.80	1102	10 516
DeltaBin044	Deltaproteobacteria	51.08	2.66	2843	95.24	11.92	441	54 886
DeltaBin048	Deltaproteobacteria	50.60	2.90	3774	77.60	38.52	1238	24 934
DeferriBin019	Deferribacteres	46.16	5.66	5252	100.00	59.31	1600	40 272
CaldiBin024	Caldilineae	58.61	5.11	4978	99.09	8.58	766	132 167
AnaeroBin020	Anaerolineae	61.54	4.25	4986	96.55	26.33	1477	26 958
AlphaBin023	Alphaproteobacteria	61.16	2.39	3062	86.31	9.04	950	16 719
AlphaBin068	Alphaproteobacteria	48.13	1.31	1697	16.25	0.86	512	23 917
ActinoBin026	Actinobacteria	71.81	2.90	3229	94.02	12.54	566	35 545

Abbreviations: Compl., completeness; Cont., contamination; OTU, operational taxonomic unit.

predominance of helical stalks (Chan *et al.*, 2016b), whereas analysis of veil-type mats showed a prevalence of the sheathed morphology (Fleming *et al.*, 2013).

A comprehensive community fingerprint analysis by T-RFLP of 25 mat communities from seven vent sites showed three distinct groups, which corresponded to the gross mat morphology of curds, veils and streamers (Figure 3); however, these groups did not correlate with location or site temperature. All of the microbial mats were collected with a Biomat Syringe sampler, allowing for precision sampling of the topmost active layer of the mat. The morphology of Group I mats are characterized as light yellow to light orange curds, Group II are yellow veiled-type mats and Group III are comprised of white to dark orange streamers attached to the vent orifice. Group I mats had the greatest abundance (56.3% ± 15.5%) of Zetaproteobacteria within the bacterial community, whereas Group II had significantly less Zetaproteobacteria (20.5% ± 2.7%) and Group III had the lowest (17.7% ± 13.7%) as determined by qPCR.

SSU rRNA gene clone libraries were constructed from representative mat communities in an attempt to identify the microbial community members driving the T-RFLP clustering. Group I mats had a lower bacterial diversity compared to the other two groups, and exhibited high levels of zOTUs 1 and 2. Group II mats contained a higher abundance of zOTUs 4, 6 and 10 along with Gammaproteobacteria. Group III mats were dominated by sulfur- and hydrogen-metabolizing Epsilonproteobacteria, with a smaller contribution from zOTUs. These results highlight a clear difference between Fe-rich (Groups I and II) and S-rich (Group III) habitats, and between direct flow (Groups I and III) and indirect/diffuse-flow (Group II) environments (Figures 2 and 3; Supplementary Figures 1 and 2).

Assembly and annotation

Six samples, two representatives from each morphotype group, were chosen for metagenomic sequencing. The resulting composite assembly had 162 376 contigs comprised of 289 114 522 bases with an overall GC% of 51.1% and an n50 of 3483. This composite assembly was separated into genome bins based on coverage and tetranucleotide frequencies of the scaffolds with MaxBin 2.0. These bins contained 77.9% of the total composite metagenome bases and 37.4% of the scaffolds. There were no sequences in multiple bins. Genome binning of the composite metagenome resulted in 93 total bins. These genome bins were assessed for completeness and taxonomic classification using CheckM (Parks *et al.*, 2015). Two of the bins were identified as Archaea, which is consistent with previous analysis showing Archaea were either below the detection limit or less than 5% of the community, and generally derived from deep-sea archaeoplankton retention in the mats (Moyer

et al., 1998; Rassa *et al.*, 2009). Nine genomes were unresolved to the class level; however, one of these bins contained a full-length SSU rRNA gene identified as a Deferribacteres (LoihiBin_014). Unclassified bins were removed from further analysis. The most numerous genome bins identified belonged to the Zetaproteobacteria (Table 1). Overall, the bins had an average n50 of 12 376 in an average of 707 scaffolds. The genome bins range in completeness from 6.55 to 100%, with an average of 70.8% (±30.8%). Contamination ranged from 0.0 to 83%, with an average of 12.6% (±15.0%). On average, the Zetaproteobacteria genome bins were 62.9% (±34.1%) complete, with an average contamination level of 11.6% (±13.4%).

T-RFLP and qPCR results both indicate that Group I mat communities were less diverse than Group II or Group III. This is again corroborated by coverage analysis of the genome bins, where communities from Group I have the lowest diversity and Group III had the highest diversity. Zetaproteobacteria genome bins were still present, though as minor community members, in the representative Group III communities (Figure 4). Group III also had higher coverage estimates within the Nitrospira, Gamma-, Epsilon- and Alphaproteobacteria. Zetaproteobacteria genome bins had the highest coverage in the Group I mat communities. The bacterial taxa distribution observed in the clone libraries is consistent with that estimated by genome binning from metagenomics (Figure 4; Supplementary Figure 1).

Carbon utilization

All isolates of Zetaproteobacteria grow via lithoautotrophy and encode for the RubisCO protein for carbon fixation from CO_2. *Mariprofundus ferrooxydans* PV-1, *M. ferrooxydans* JV-1, *M. ferrooxydans* M34 and *Mariprofundus* DIS-1 encode for both Form I and Form II large subunit RubisCO gene, whereas *Zetaproteobacterium* TAG-1 and *Mariprofundus* sp. EFK-M39 only encodes a Form II RubisCO (Field *et al.*, 2015). In total, 87 genes were identified as the large subunit of RubisCO. Of these, 67 were Form II and 11 were Form I. Of the Form I genes, only one was binned into a Zetaproteobacteria genome bin (ZetaBin022). The majority of the RubisCO Form II genes belonged to Zetaproteobacteria and 28 of the Zetaproteobacteria genome bins encoded a Form II gene, including the bin with the Form I gene (ZetaBin022). The Gammaproteobacteria had the second highest abundance of RubisCO genes, with four Form I and sixteen Form II genes detected. Twenty-three of the RubisCO genes were not placed into genome bins, but nine of these had the highest similarity to Zetaproteobacteria genes and six were most similar to Gammaproteobacteria (Supplementary Table 5).

In comparison, only seven ATP citrate lyase (encoded by *aclB*) genes were identified. This is a key gene in the reductive tricarboxylic acid cycle
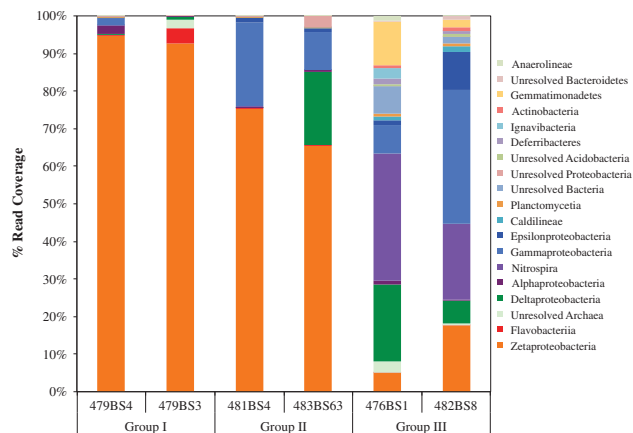
Figure 4 Relative abundance estimated by read coverage of taxonomically-classified genome bins from the sampled microbial communities. Genome bins were assessed for taxonomic classification using CheckM.

and is found in autotrophic Epsilonproteobacteria and Aquifacales (Hügler and Sievert, 2011). Five of the seven *aclB* genes were binned into Epsilonproteobacteria genome bins (Supplementary Table 6). The closest taxonomic hits were to *Sulfurovum* sp AR, *Sulfurimonas autotrophica* OK10 and *Nitratiruptor* sp SB155-2. Two of these organisms, *S. autotrophica* OK10 and Nitratiruptor sp. SB155-2, were isolated from Iheya North hydrothermal field sediments and chimneys, respectively (Sikorski *et al.*, 2010; Inoue *et al.*, 2016). *Sulfurovum* sp. AR was isolated from deep marine sediments collected near Svalbard, within the Arctic Circle (Park *et al.*, 2012).

There was a high diversity of Form II RubisCO proteins recovered from Zetaproteobacteria genome bins and unbinned proteins identified as Zetaproteobacteria by IMG (Figure 5; Supplementary Table 5). Many of these RubisCO proteins were most similar to RubisCO proteins from the Zetaproteobacteria SAGs belonging to zOTU 2. This zOTU was one of the two considered as cosmopolitan because it is found throughout the Pacific Ocean (McAllister *et al.*, 2011).

Targeted qPCR on RubisCO Form II (*cbbM*) showed high abundance of the gene correlated strongly with a high abundance of Zetaproteobacteria (Jesser *et al.*, 2015). The abundance of Form II RubisCO genes in comparison to Form I is indicative of adaptations to high CO_2 and very low O_2 environments (Hernandez *et al.*, 1996; Tabita *et al.*, 2008). The prevalence of Form II RubisCO in the genome bins of the Zetaproteobacteria (Table 2) shows an adaptation to growth in very low O_2 environments similar to what is found in and around Pele's Pit (Glazer and Rouxel, 2009). Zetaproteobacteria SAGs showed a similar pattern, in that Form I RubisCO was undetected (Field *et al.*, 2015). Only a single Zetaproteobacteria genome bin contained both forms of RubisCO, suggesting that genotypes containing only Form II are the most prevalent.

Nitrogen cycling
Biological nitrogen fixation is a key process in any ecosystem. The gene *nifH* encodes the nitrogenase reductase subunit, and is commonly used to track abundance and diversity among nitrogen-fixing organisms (Gaby and Buckley, 2012). Of the Zetaproteobacteria, *Mariprofundus* sp. EKF-M39, DIS-1 and *M. ferrooxydans* M34 encode a *nifH* gene, and qPCR estimates showed very low occurrence of *nifH* in microbial mat communities from Lōʻihi Seamount (Jesser *et al.*, 2015). Consistent with this notion, only eleven *nifH* genes were identified and only two of these were within Zetaproteobacteria genome bins (ZetaBin035 & ZetaBin089). ZetaBin089 also encodes for *nifD* and *nifK*, the nitrogenase alpha and beta subunits, respectively. These genes are encoded on the same contig and are syntenous with the other identified *nifH*-containing Zetaproteobacteria isolates (Supplementary Figure 3). ZetaBin035 is lacking the alpha and beta subunits, but encodes the dinitrogenase iron-molybdenum cofactor, which is involved in the synthesis of the iron-molybdenum cofactor that binds the active site of the nitrogenase enzyme. Based on these annotations, it appears that these two Zetaproteobacteria bins (ZetaBin035 and ZetaBin089) are potentially capable of nitrogen fixation.

Diverse *nifH* genes have been identified at Axial Seamount, located along the Juan de Fuca Ridge (Mehta *et al.*, 2003) and interestingly, ammonium has been detected to similar levels as found at Lōʻihi microbial mats, where *nifH* genes were either below detection or at very low abundance (Jesser *et al.*, 2015). Ammonium transport proteins (*amt*) were found in 26 of the Zetaproteobacteria genome bins, including the genome bins that encode a *nifH* (Table 2). Use of nitrate and/or nitrite as a nitrogen source appears to be the most common across the Zetaproteobacteria genome bins. The majority of the Zetaproteobacteria genome bins contained genes for nitrate reduction (*nasAB*) and/or nitrite reductase (*nirBD*) for the assimilation of nitrogen. The dissimilatory nitrate reductase (*napAB*) and nitrite reductase (*nirK/nirS*) were also identified in 18 of the Zetaproteobacteria genome bins (Table 2) showing that denitrification is also possible. The prevalence of the ammonium transport proteins, presence of assimilatory nitrogen pathways, and the low recovery of *nifH* suggest that Zetaproteobacteria rely more on the presence of bioavailable nitrogen compounds accessed from the environment, rather than by dinitrogen fixation.

Arsenic cycling
Arsenic has been found at hydrothermal vents and the arsenic detoxification gene, arsenate reductase
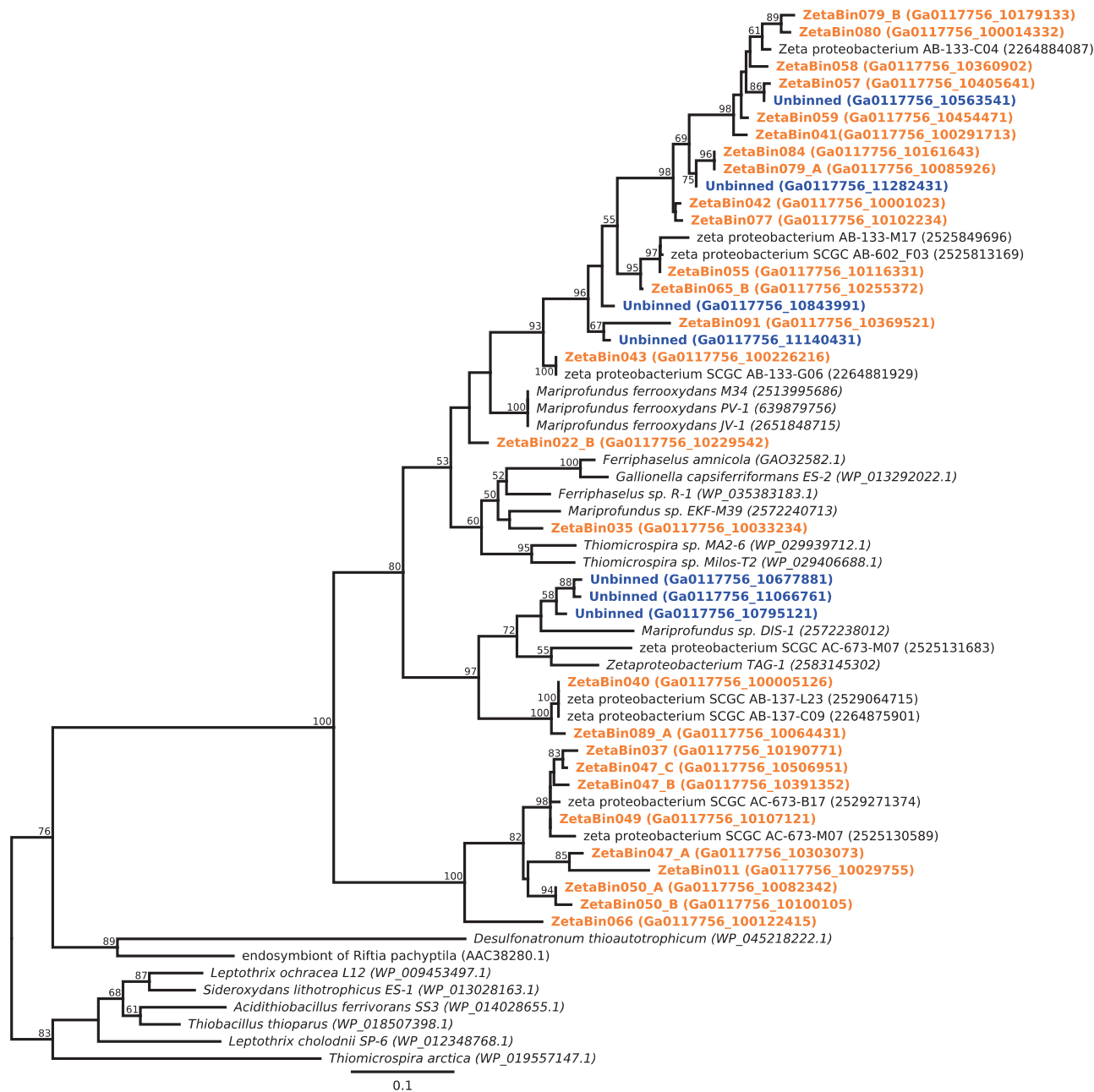
Figure 5 RAxML phylogenetic tree of the Form II RubisCO proteins from Zetaproteobacteria genome bins (orange) and unbinned proteins identified as Zetaproteobacteria by IMG (blue). Numbers within parenthesis are gene identification numbers. Bootstrap values (⩾50) are representative of 1000 iterations.

(encoded by *arsC*) has been identified in abundance in microbial mats from Lōʻihi hydrothermal habitats (Jesser *et al.*, 2015). ArsC reduces arsenate to arsenite, which can then be exported from the cell via an arsenite specific transporter. In the composite assembly, there were 195 identified *arsC* genes in 67 of the genome bins representing every taxonomic class. The majority of the binned *arsC* genes were contained within either the Zetaproteobacteria or Gammaproteobacteria genome bins, with 71 and 28 gene copies, respectively. Of the identified *arsC* genes that were unbinned, taxonomic placement by

IMG shows these genes to again be similar to genes from Zetaproteobacteria and Gammaproteobacteria. Arsenite transport proteins were identified in 23 of the Zetaproteobacteria genome bins. All of the Zetaproteobacteria genome bins with an arsenite transport protein contained an arsenate reductase as well.

At Tutum Bay, a shallow water hydrothermal vent system, ~ 1.5 kg of arsenic per day is released into the environment (Meyer-Dombard *et al.*, 2013). This system also releases reduced iron, and Zetaproteobacteria were shown to heavily colonize slides

Table 2 Number of genes per Zetaproteobacteria genome bins. Bins were sorted by their closest zOTU as determined by both ANI and AAI

OTU by Closest SAG	GenomeBin	cbbM	ccoN	ccoO	coxA	cyc2 (PV-1)	cyc1 (PV-1)	arsC	nirK/ nirS	napA	narG	nasAB	nirB	nirD	nifH	amt
1	ZetaBin042	1	4	3		1	1	3	3			1	1	1		2
1	ZetaBin066	1	4	2		2	2	3	2			1	1	1		2
1	ZetaBin077	1	6	4	1		2	3				1	2	1		2
1	ZetaBin079	2	4	2			1	3	1			1	2	1		2
1	ZetaBin080	1	4	2		1	1	3				1	1	1		2
1	ZetaBin084	1	6	2	1	5	2	4	5	1	2	2	5	2		7
1	ZetaBin088		5	4	1	2	2	6	2			3	2			2
1	ZetaBin092		3					3	2	3		2	1	1		2
1	ZetaBin041	1	3	1		1	1	3	5			1	1	1		2
1	ZetaBin043	1	4	2		1	1	3	1	1		1	1	1		1
2	ZetaBin052		1					1								
2	ZetaBin055	1	1				1	3								
2	ZetaBin056		1	1			1	1								1
2	ZetaBin057	1	1					1								
2	ZetaBin058	1						1				1	1	1		
2	ZetaBin059	1	4	2		1	1	2				2	1	1		2
2	ZetaBin060					1										
2	ZetaBin062		3	3		1						1				3
2	ZetaBin064		3	1		1			4			1	1			
2	ZetaBin065	2	4	2		2	2	5								5
2	ZetaBin069					1		1								
2	ZetaBin078															1
2	ZetaBin090		3	3		3		3		2		3	1	1		
4	ZetaBin030															
4	ZetaBin047	3	3		3		1	2	1				2	1		6
4	ZetaBin037	1			1	1		2	1					1		2
4	ZetaBin050	2	3	2	2	2	1	4					2			4
6	ZetaBin040	1	3	1		1	1	3	1	1		1	1	1		3
9	ZetaBin089	2	5	1	2	2	1	2	1	1		4	2		1	12
9	ZetaBin091	1	3	1		1	1			1		2	1	1		1
10	ZetaBin049	1	2	1	3	5		1					1	1		1
11	ZetaBin011	1	3	1	2	2	1	2	1				2	1		2
11	ZetaBin022	2	2		2			1	2			1	2	1		2
11	ZetaBin035	1	3	1		4		2		1			3		1	2
Bin Total	34	23	28	22	10	22	19	28	15	8	1	19	23	19	2	25
Gene totals		30	91	42	18	41	24	71	32	11	2	30	37	20	2	71

Abbreviations: AAI, average amino acid identity; ANI, average nucleotide identity; OTU, operational taxonomic unit; SAG, single amplified genomes; zOTU, zetaproteobacteria OTU.

incubated *in situ*. Although arsenic geochemistry has yet to be recorded at Lō'ihi vents, the abundance of arsenic-related genes found in our composite assembly suggests that arsenate is abundant in this environment. However, to show this, further geochemical analysis targeting arsenic redox states at Lō'ihi would be required.

Electron transport chain
Zetaproteobacteria SAGs and isolate genomes encode for a cbb$_3$-type cytochrome c oxidase (Field *et al.*, 2015; Fullerton *et al.*, 2015). *M. ferrooxydans* PV-1, encodes for subunits I–III (*ccoNOP*) and appears to be lacking subunit IV (*ccoQ*) according to Singer *et al.* (2011). Only the CcoNO subunits were identified in the proteomic profile of *M. ferrooxydans* PV-1 (Barco *et al.*, 2015). Eleven of the 34 Zetaproteobacteria bins encode all four subunits of the cbb$_3$-type cytochrome c oxidase. *Mariprofundus* sp. EKF-M39, DIS-1, *M. ferrooxydans*

JV-1 and six of the Zetaproteobacteria SAGs encode all four subunits of the cbb$_3$-type cytochrome c oxidase. Nine of the Zetaproteobacteria genome bins encode for subunits I–III and appear to lack subunit IV. The *ccoQ* gene product is a membrane-spanning protein of unclear function; *ccoN* gene encodes for the catalytic subunit and *ccoO,* a monoheme c-type cytochrome. Only the *ccoNO* subunits are common to all gene clusters across multiple bacterial phyla (Ducluzeau *et al.*, 2008).

The cbb$_3$-type cytochrome c oxidase has a high affinity for O$_2$ and is predominantly used under microaerophilic conditions and may also be used to prevent O$_2$ poisoning (Sievert *et al.*, 2008; Jewell *et al.*, 2016). The aa$_3$-type cytochrome c oxidase is encoded by *coxABC* where expression is repressed in facultative anaerobes under low oxygen conditions (Pitcher and Watmough, 2004). Ten of the Zetaproteobacteria genome bins contain the *coxA* gene (aa$_3$-type cytochrome c oxidase), and all but one of these genome bins encodes for the

1910

ccoNOP (cbb$_3$-type cytochrome c oxidase) as well. This suggests that like other facultative anaerobes and microaerophiles, Zetaproteobacteria are able to modulate their electron transport chain to account for variable oxygen conditions. Only one of the 24 Zetaproteobacteria SAGs encodes both types of the cytochrome c oxidases (Field *et al.*, 2015).

There is no direct evidence that Zetaproteobacteria can grow anaerobically using nitrate as the terminal electron acceptor; however, a number of other iron-oxidizing Proteobacteria can grow anaerobically this way (Hedrich *et al.*, 2011; Beller *et al.*, 2013). In the Zetaproteobacteria genome bins there was one bin, ZetaBin084, which encoded the respiratory nitrate reductase, NarG. This genome bin also encodes the cbb$_3$ and aa$_3$ type cytochrome c oxidases, that is, both the *ccoNO* and *coxA* genes.

Iron oxidation is hypothesized to occur on the outer membrane and is coupled to cytoplasmic and membrane-bound electron transfer proteins (Hedrich *et al.*, 2011; Ilbert and Bonnefoy, 2013). From *M. ferrooxydans* PV-1 genome analysis, a molybdopterin oxidoreductase (Mob, SPV1_03948) was hypothesized to be important in Fe(II) oxidation (Singer *et al.*, 2011), and showed synteny with two contigs contained in a fosmid library generated from a suction-sample collected from Hiolo South (Singer *et al.*, 2013). This protein was also identified in the top 25 most abundant proteins of *M. ferrooxydans* PV-1; however, its function in iron oxidation is questionable due to high similarity to proteins found in non-iron oxidizers (Barco *et al.*, 2015). In the Zetaproteobacteria genome bins, similar proteins were detected and annotated by IMG as different molybdopterin-containing oxidoreductases (for example, nitrate reductase NapA; Supplementary Table 4).

Proteomic analysis of *M. ferrooxydans* PV-1 revealed a membrane bound cytochrome that was highly expressed and distantly related to cytochrome c$_2$ of *Acidothiobacillus ferrooxydans* (Barco *et al.*, 2015; White *et al.*, 2016). It has been proposed that this protein, referred to as Cyc2$_{PV-1}$, is the site of electron transfer from iron to a cytoplasmic cytochrome (Cyc1$_{PV-1}$), which was also identified as high-abundant by proteomic analysis. From Cyc1$_{PV-1}$, electrons are hypothesized to be shuttled into a membrane-bound electron transport chain, terminating with the cbb$_3$-type cytochrome c oxidase. Using the amino acid sequence of Cyc1$_{PV-1}$ and Cyc2$_{PV-1}$ to search the composite metagenome, 24 and 41 gene copies, respectively, were identified within the Zetaproteobacteria genome bins (Table 2). The open reading frames most similar to Cyc1$_{PV-1}$ were annotated as cytochrome c553, whereas the Cyc2$_{PV-1}$ genes were annotated as hypothetical proteins by IMG (Supplementary Tables 2 and 3). The identification of Cyc1$_{PV-1}$ and Cyc2$_{PV-1}$ in our Zetaproteobacteria genome bins, supports the hypothesis that a Cyc2-like protein is the site of iron oxidation, as opposed to the alternative hypothesis using the Mob protein (Hedrich *et al.*, 2011; Singer *et al.*, 2011; Ilbert and Bonnefoy, 2013; Barco *et al.*, 2015). These Cyc2-like proteins were identified in every zOTU detected, indicating their ubiquity across the Zetaproteobacteria, including within the ecologically significant taxa (Table 2).

Whole genome comparisons
In this composite metagenome study, there were 249 total SSU rRNA genes recovered. Of these, 41 were contained within Zetaproteobacteria genome bins as determined by CheckM and 37 SSU rRNA genes were identified as Zetaproteobacteria by the RDP classifier (Wang *et al.*, 2007; Parks *et al.*, 2015). Previous studies on Zetaproteobacteria SSU rRNA diversity identified two operational taxonomic units that were ubiquitous across the Pacific Ocean, referred to as zOTUs 1 and 2 (McAllister *et al.*, 2011). Genomes were compared at the nucleotide level to assess genomic diversity across the Zetaproteobacteria genome bins as compared to isolate genomes and SAGs (Figure 6) by ANI. Hierarchical clustering of the genomes based on ANI showed that genome bins most similar to zOTUs 1 and 2 are the most highly represented, with 10 and 13 out of the 34 Zetaproteobacteria genome bins, respectively. Based on Form II RubisCO phylogeny, these zOTUs constitute a single lineage that diverged more recently than any of those that occurred in other lineages (Figure 5). Both these zOTUs were also found to be the most abundant phylotypes detected in microbial mats from Lō'ihi hydrothermal habitats by SAGs and SSU clone library analyses (McAllister *et al.*, 2011; Field *et al.*, 2015). Based on the cluster analysis of ANI comparisons from our Zetaproteobacteria genome bins, this study has shown that zOTU 2 represents a monophyletic cluster and is distinct from all the other zOTU clusters (Figure 6), and based on estimated genome size hints, that genome streamlining may be occurring within this group. This zOTU was also the first to be identified from any hydrothermal system (Moyer *et al.*, 1995). Our whole genome cluster analysis also showed that zOTUs 1, 4, 6 and 10 have much greater genomic dissimilarity (that is, diversity) than what would be expected based on SSU rRNA identity alone. The distribution of Zetaproteobacteria genome bins across the three different groups of mat communities shows that zOTU 2 is the most abundant in both Group I and Group II (that is, both curds and veils) type mats based on gross morphology, representing twisted-stalks and sheaths, respectively. The Group III mats (streamers), which have a low Zetaproteobacterial abundance relative to the other members of the community, included zOTU 11 as the most highly represented within this mat-type (Supplementary Figure 4).
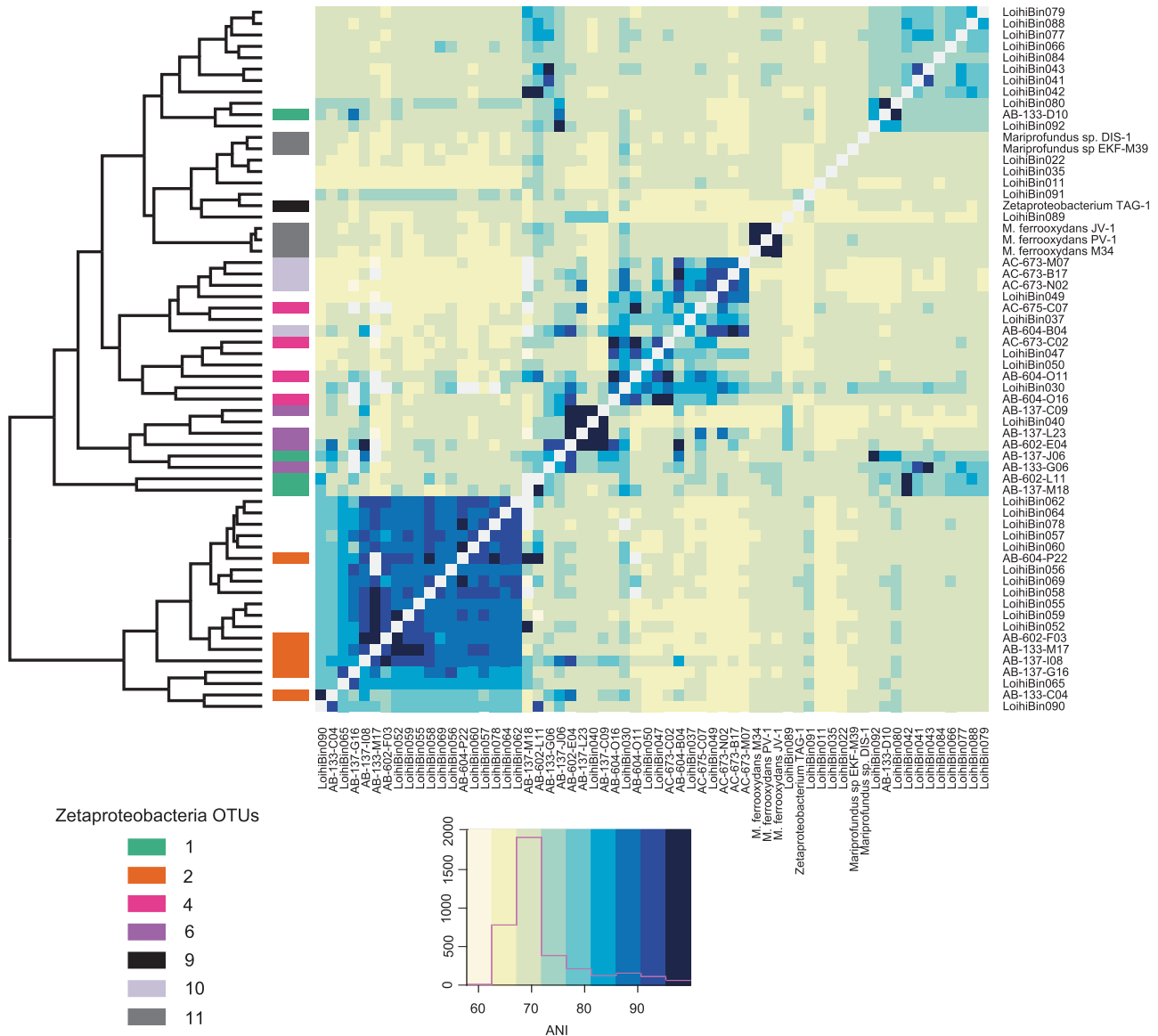
Figure 6 Hierarchical clustering heatmap and dendrogram of ANI of Zetaproteobacteria genome bins, and isolate Zetaproteobacteria genomes. Genome self-comparisons and where ANI could not be determined are presented in light gray. Genome bins were confirmed by average amino acid identity.

Using this hierarchical cluster analysis approach, patterns of metabolic potential across zOTUs can also be realized. The only two bins with a *nifH* gene (ZetaBin035 and ZetaBin089) were also most closely related to isolates that are able to fix nitrogen. All cultured isolates remain within the same tight cluster, including the type strain *M. ferrooxydans* PV-1, possibly indicating a narrow range of selection pressure resulting from our present culturing techniques. Furthermore, there were few Zetaproteobacteria genome bins with similarity to any cultured isolates, suggesting environmental parameters are poorly mimicked in the lab. In general, the RubisCO protein relationships and genome relationships identified by ANI were conserved (that is, similar). None of the genome bins within zOTU 2 contained genes for the aa$_3$-type cytochrome c oxidase, further supporting adaptation to the low O$_2$ levels found at Lō'ihi hydrothermal habitats.

Conclusions

Coverage analysis of our composite metagenome indicates that carbon is fixed primarily by Zetaproteobacteria containing Form II RubisCO. Through an assessment of the diversity of Form II RubisCO genes and the abundance of cbb$_3$-type cytochrome c oxidase genes, many Zetaproteobacteria show an adaptation to life at very low oxygen levels in conjunction with high-ferrous iron and dissolved

CO_2 levels. Denitrification is less common, and our data indicates that bioavailable nitrogen is primarily metabolized. Nearly all of the Zetaproteobacteria genome bins contain genes for the detoxification of arsenate as well as representatives from each of the other classes that were detected in these microbial mat communities. This shows that metagenomics analyses can also provide insights into geochemical conditions. The lineage represented by zOTU 2 is monophyletic suggesting an ancestral bottleneck during its more recent evolutionary history. This zOTU is also the most prevalent of our Zetaproteobacteria genome bins, indicating it is the most ecologically successful manifestation of both sheath and stalk morphology. Through the use of genome-resolved metagenomics, we have better constrained patterns observed in metabolic potential and divergence across many of the Zetaproteobacteria growing within microbial mats at Lō'ihi Seamount.

Conflict of Interest

The authors declare no conflict of interest.

Acknowledgements

References

Andrews S. (2010), FastQC: A quality control tool for high throughput sequence data. Available at: http://www.bioinformatics.babraham.ac.uk/projects/fastqc.

Beller HR, Zhou P, Legler TC, Chakicherla A, Kane S, Letain TE *et al.* (2013). Genome-enabled studies of anaerobic, nitrate-dependent iron oxidation in the chemolithoautotrophic bacterium *Thiobacillus denitrificans. Front Microbiol* **4**: 249.

Barco RA, Emerson D, Sylvan JB, Orcutt BN, Meyers MEJ, Ramírez GA *et al.* (2015). New insight into microbial iron oxidation as revealed by the proteomic profile of an obligate iron-oxidizing chemolithoautotroph. *Appl Environ Microbiol* **81**: 5927–5937.

Chan CS, Emerson D, Luther GW III. (2016a). The role of microaerophilic Fe-oxidizing micro-organisms in producing banded iron formations. *Geobiology* **14**: 509–528.

Chan CS, Fakra SC, Emerson D, Fleming EJ, Edwards KJ. (2011). Lithotrophic iron-oxidizing bacteria produce organic stalks to control mineral growth: implications for biosignature formation. *ISME J* **5**: 717–727.

Chan CS, McAllister SM, Leavitt AH, Glazer BT, Krepski ST, Emerson D. (2016b). The architecture of iron microbial mats reflects the adaptation of chemolithotrophic iron oxidation in freshwater and marine environments. *Front Microbiol* **7**: 796.

Davis RE, Moyer CL. (2008). Extreme spatial and temporal variability of hydrothermal microbial mat communities along the Mariana Island Arc and southern Mariana back-arc system. *J Geophys Res* **113**: B08S15.

Druschel GK, Emerson D, Sutka R, Suchecki P, Luther GW III. (2008). Low-oxygen and chemical kinetic constraints on the geochemical niche of neutrophilic iron (II) oxidizing microorganisms. *Geochim Cosmochim Acta* **72**: 3358–3370.

Ducluzeau A-L, Ouchane S, Nitschke W. (2008). The cbb_3 oxidases are an ancient innovation of the domain bacteria. *Mol Biol Evol* **25**: 1158–1166.

Emerson D, Rentz JA, Lilburn TG, Davis RE, Aldrich H, Chan CS *et al.* (2007). A novel lineage of *Proteobacteria* involved in formation of marine Fe-oxidizing microbial mat communities. *PLoS One* **2**: e667.

Emerson D, Moyer CL. (2010). Microbiology of Seamounts: common patterns observed in community structure. *Oceanography* **23**: 148–163.

Emerson D, Field EK, Chertkov O, Davenport KW, Goodwin L, Munk C *et al.* (2013). Comparative genomics of freshwater Fe-oxidizing bacteria: implications for physiology, ecology, and systematics. *Front Microbiol* **4**: 254.

Field EK, Kato S, Findlay AJ, MacDonald DJ, Chiu BK, Luther GW III *et al.* (2016). Planktonic marine iron oxidizers drive iron mineralization under low-oxygen conditions. *Geobiology* **14**: 499–508.

Field EK, Sczyrba A, Lyman AE, Harris CC, Woyke T, Stepanauskas R *et al.* (2015). Genomic insights into the uncultivated marine Zetaproteobacteria at Loihi Seamount. *ISME J* **9**: 857–870.

Fleming EJ, Davis RE, McAllister SM, Chan CS, Moyer CL, Tebo BM *et al.* (2013). Hidden in plain sight: discovery of sheath-forming, iron-oxidizing *Zetaproteobacteria* at Loihi Seamount, Hawaii, USA. *FEMS Microbiol Ecol* **85**: 116–127.

Fullerton H, Hager KW, Moyer CL. (2015). Draft genome sequence of *Mariprofundus ferrooxydans* strain JV-1, isolated from Loihi Seamount, Hawaii. *Genome Announc* **3**: e01118–15.

Gaby JC, Buckley DH. (2012). A comprehensive evaluation of PCR primers to amplify the nifH gene of nitrogenase. *PLoS One* **7**: e42149.

Glazer BT, Rouxel OJ. (2009). Redox speciation and distribution within diverse iron-dominated microbial habitats at Loihi Seamount. *Geomicrobiol J* **26**: 606–622.

Guilbaud R, Poulton SW, Butterfield NJ, Zhu M, Shields-Zhou GA. (2015). A global transition to ferruginous conditions in the early Neoproterozoic oceans. *Nat Geosci* **8**: 466–470.

Hedrich S, Schlömann M, Johnson DB. (2011). The iron-oxidizing proteobacteria. *Microbiol* **157**: 1551–1564.

Hernandez JM, Baker SH, Lorbach SC, Shively JM, Tabita FR. (1996). Deduced amino acid sequence, functional expression, and unique enzymatic properties of the form I and form II ribulose bisphosphate carboxylase/oxygenase from the chemoautotrophic bacterium *Thiobacillus denitrificans*. *J Bacteriol* **178**: 347–356.

Holland HD. (2006). The oxygenation of the atmosphere and oceans. *Phil Trans R Soc Lond B Biol Sci* **361**: 903–915.

Hügler M, Sievert SM. (2011). Beyond the Calvin cycle: autotrophic carbon fixation in the ocean. *Ann Rev Mar Sci* **3**: 261–289.

Ilbert M, Bonnefoy V. (2013). Insight into the evolution of the iron oxidation pathways. *Biochim Biophys Acta* **1827**: 161–175.

Inoue A, Anraku M, Nakagawa S, Ojima T. (2016). Discovery of a novel alginate lyase from *Nitratiruptor* sp. SB155-2 thriving at deep-sea hydrothermal vents and identification of the residues responsible for its heat stability. *J Biol Chem* **291**: 15551–15563.

Jesser KJ, Fullerton H, Hager KW, Moyer CL. (2015). Quantitative PCR analysis of functional genes in iron-rich microbial mats at an active hydrothermal vent system (Lōʻihi Seamount, Hawaiʻi). *Appl Environ Microbiol* **81**: 2976–2984.

Jewell TN, Karaoz U, Brodie EL, Williams KH, Beller HR. (2016). Metatranscriptomic evidence of pervasive and diverse chemolithoautotrophy relevant to C, S, N and Fe cycling in a shallow alluvial aquifer. *ISME J* **10**: 2106–2117.

Kearse M, Moir R, Wilson A, Stones-Havas S, Cheung M, Sturrock S *et al.* (2012). Geneious Basic: An integrated and extendable desktop software platform for the organization and analysis of sequence data. *Bioinformatics* **28**: 1647–1649.

Konhauser KO, Newman DK, Kappler A. (2005). The potential significance of microbial Fe (III) reduction during deposition of Precambrian banded iron formations. *Geobiology* **3**: 167–177.

Langmead B, Salzberg SL. (2012). Fast gapped-read alignment with Bowtie 2. *Nat Methods* **9**: 357–359.

Martin M. (2011). Cutadapt removes adapter sequences from high-throughput sequencing reads. *EMBnet J* **17**: 10–12.

McAllister SM, Davis RE, McBeth JM, Tebo BM, Emerson D, Moyer CL. (2011). Biodiversity and emerging biogeography of the neutrophilic iron-oxidizing *Zetaproteobacteria*. *Appl Environ Microbiol* **77**: 5445–5457.

Mehta MP, Butterfield DA, Baross JA. (2003). Phylogenetic diversity of nitrogenase (*nifH*) genes in deep-sea and hydrothermal vent environments of the Juan de Fuca Ridge. *Appl Environ Microbiol* **69**: 960–970.

Meyer-Dombard DAR, Amend JP, Osburn MR. (2013). Microbial diversity and potential for arsenic and iron biogeochemical cycling at an arsenic rich, shallow-sea hydrothermal vent (Tutum Bay, Papua New Guinea). *Chem Geol* **348**: 37–47.

Moyer CL, Dobbs FC, Karl DM. (1995). Phylogenetic diversity of the bacterial community from a microbial mat at an active, hydrothermal vent system, Loihi Seamount, Hawaii. *Appl Environ Microbiol* **61**: 1555–1562.

Moyer CL, Tiedje JM, Dobbs FC, Karl DM. (1998). Diversity of deep-sea hydrothermal vent *Archaea*. *Deep Sea Res II* **45**: 303–317.

Park S-J, Ghai R, Martín-Cuadrado A-B, Rodríguez-Valera F, Jung M-Y, Kim J-G *et al.* (2012). Draft genome sequence of the sulfur-oxidizing bacterium 'Candidatus Sulfurovum sediminum' AR, which belongs to the *Epsilonproteobacteria*. *J Bacteriol* **194**: 4128–4129.

Parks DH, Imelfort M, Skennerton CT, Hugenholtz P, Tyson GW. (2015). CheckM: assessing the quality of microbial genomes recovered from isolates, single cells, and metagenomes. *Genome Res* **25**: 1043–1055.

Peng Y, Leung HCM, Yiu SM, Chin FYL. (2012). IDBA-UD: a *de novo* assembler for single-cell and metagenomic sequencing data with highly uneven depth. *Bioinformatics* **28**: 1420–1428.

Pitcher RS, Watmough NJ. (2004). The bacterial cytochrome cbb_3 oxidases. *Biochim Biophys Acta* **1655**: 388–399.

Planavsky N, Rouxel O, Bekker A, Shapiro R, Fralick P, Knudsen A. (2009). Iron-oxidizing microbial ecosystems thrived in late Paleoproterozoic redox-stratified oceans. *Earth Planet Sci Lett* **286**: 230–242.

Rassa AC, McAllister SM, Safran SA, Moyer CL. (2009). *Zeta-Proteobacteria* dominate the colonization and formation of microbial mats in low-temperature hydrothermal vents at Loihi Seamount, Hawaii. *Geomicrobiol J* **26**: 623–638.

Raven JA, Evans MCW, Korb RE. (1999). The role of trace metals in photosynthetic electron transport in O_2-evolving organisms. *Photosyn Res* **60**: 111–149.

Resing JA, Sedwick PN, German CR, Jenkins WJ, Moffett JW, Sohst BM *et al.* (2015). Basin-scale transport of hydrothermal dissolved metals across the South Pacific Ocean. *Nature* **523**: 200–203.

Rodriguez-R LM, Konstantinidis KT. (2016). The enveomics collection: a toolbox for specialized analyses of microbial genomes and metagenomes. *PeerJ Preprints* **4**: e1900v1. Available at: https://doi.org/10.7287/peerj.preprints.1900v1.

Richter M, Rosselló-Móra R. (2009). Shifting the genomic gold standard for the prokaryotic species definition. *Proc Natl Acad Sci USA* **106**: 19126–19131.

Scott JJ, Breier JA, Luther GW III, Emerson D. (2015). Microbial iron mats at the Mid-Atlantic Ridge and evidence that Zetaproteobacteria may be restricted to iron-oxidizing marine systems. *PLoS One* **10**: e0119284.

Sedwick PN, McMurtry GM, Macdougall JD. (1992). Chemistry of hydrothermal solutions from Pele's Vents, Loihi Seamount, Hawaii. *Geochim Cosmochim Acta* **56**: 3643–3667.

Sievert SM, Scott KM, Klotz MG, Chain PS, Hauser LJ, Hemp J *et al.* (2008). Genome of the epsilonproteobacterial chemolithoautotroph *Sulfurimonas denitrificans*. *Appl Environ Microbiol* **74**: 1145–1156.

Sievert SM, Vetriani C. (2012). Chemoautotrophy at deep-sea vents: past, present, and future. *Oceanography* **25**: 218–233.

Sikorski J, Munk C, Lapidus A, Djao ODN, Lucas S, Del Rio TG *et al.* (2010). Complete genome sequence of *Sulfurimonas autotrophica* type strain (OK10^T). *Stand Genomic Sci* **3**: 194–202.

1914

Singer E, Emerson D, Webb EA, Barco RA, Kuenen JG, Nelson WC et al. (2011). *Mariprofundus ferrooxydans* PV-1 the first genome of a marine Fe(II) oxidizing Zetaproteobacterium.*PLoS One* **6**: e25386.

Singer E, Heidelberg JF, Dhillon A, Edwards KJ. (2013). Metagenomic insights into the dominant Fe (II) oxidizing *Zetaproteobacteria* from an iron mat at Lō´ihi, Hawai´i. *Front Microbiol* **4**: 52.

Tabita FR, Satagopan S, Hanson TE, Kreel NE, Scott SS. (2008). Distinct form I, II, III, and IV Rubisco proteins from the three kingdoms of life provide clues about Rubisco evolution and structure/function relationships. *J Exp Bot* **59**: 1515–1524.

Wang Q, Garrity GM, Tiedje JM, Cole JR. (2007). Naïve Bayesian classifier for rapid assignment of rRNA sequences into the new bacterial taxonomy. *Appl Environ Microbiol* **73**: 5261–5267.

Wheat CG, Jannasch HW, Plant JN, Moyer CL, Sansone FJ, McMurtry GM. (2000). Continuous sampling of hydrothermal fluids from Loihi Seamount after the 1996 event. *J Geophys Res* **105**: 19353–19367.

White GF, Edwards MJ, Gomez-Perez L, Richardson DJ, Butt JN, Clarke TA. (2016). Mechanisms of bacterial extracellular electron exchange. *Adv Microb Physiol* **68**: 87–138.

Wu Y-W, Simmons BA, Singer SW. (2016). MaxBin 2.0: an automated binning algorithm to recover genomes from multiple metagenomic datasets. *Bioinformatics* **32**: 605–607.

Supplementary Information accompanies this paper on The ISME Journal website (http://www.nature.com/ismej)